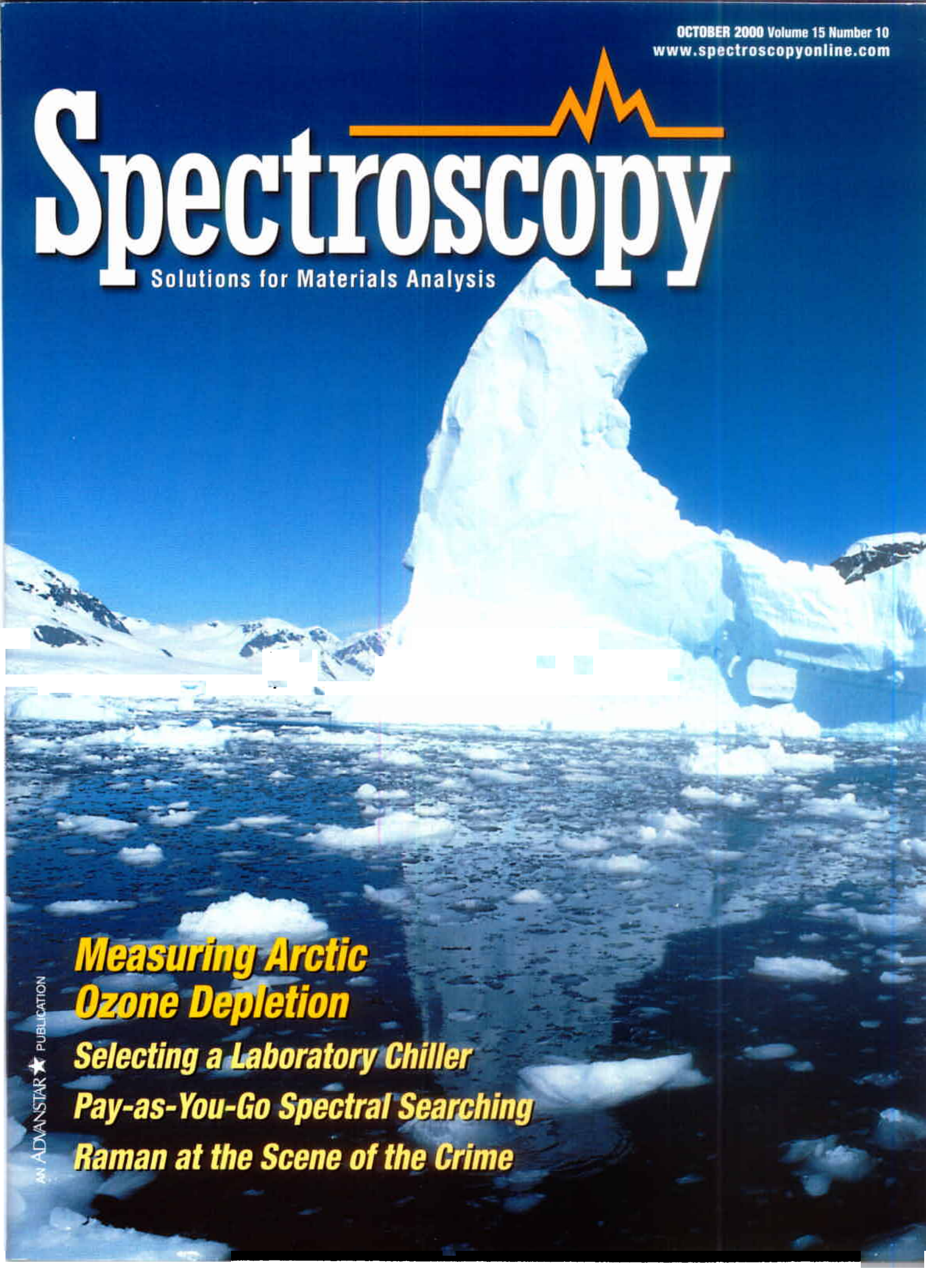


OCTOBER 2000 Volume 15 Number 10
www.spectroscopyonline.com

Spectroscopy



Solutions for Materials Analysis

***Measuring Arctic
Ozone Depletion***

Selecting a Laboratory Chiller

Pay-as-You-Go Spectral Searching

Raman at the Scene of the Crime

AN ADVANSTAR PUBLICATION

An Automated Spectrometer

for Monitoring Arctic Ozone Depletion

**Matthew R. Bassford and
Kimberly Strong***

Department of Physics
University of Toronto
Toronto, Ontario, Canada

Jagdish Rebello

JY Horiba
Edison, NJ

*Corresponding author

A portable spectrometer system has been developed for performing stand-alone measurements of stratospheric ozone and other gases important in elucidating the science behind ozone depletion. The authors describe the construction of the ground-based system and present results from a recent Arctic field campaign.



Environment Canada's Arctic Stratospheric Observatory (ASTRO) has been in operation since January 1993 for the purpose of studying the ozone layer over the Canadian High Arctic. ASTRO is located on Ellesmere Island, and is 15 km from Eureka, Nunavut, a remote weather station less than 1000 km from the North Pole.

Ozone (O_3) is naturally present in the Earth's atmosphere and is most abundant at altitudes between 20 and 25 km, in a region of the atmosphere referred to as the stratosphere. The ozone layer is important because of its critical role in absorbing harmful ultraviolet (UV)-B radiation from the sun. Consequently, the discovery of the Antarctic ozone hole (1) and observed ozone losses at other latitudes was of immense concern because of the threat to life on Earth's surface. Marine ecosystems are particularly sensitive to UV-B radiation and there is a demonstrable link between polar ozone depletion and reductions in phytoplankton population (2).

In addition to ozone destruction over the Antarctic, recent measurements have revealed substantial springtime losses in Arctic ozone columns (3). Arctic ozone depletion is a seasonal effect that begins when high-altitude ice clouds (polar stratospheric clouds) are formed during the cold polar winter. With returning sunlight, photochemical ozone loss is stimulated by the presence of active halogen atoms such as Cl. Nitrogen compounds — in particular NO_2 — also play a part in regulating ozone concentrations by sequestering active halogen species, such as ClO, into less reactive forms like $ClONO_2$. However, in contrast to the Antarctic, the relative importance of processes governing Arctic ozone loss is

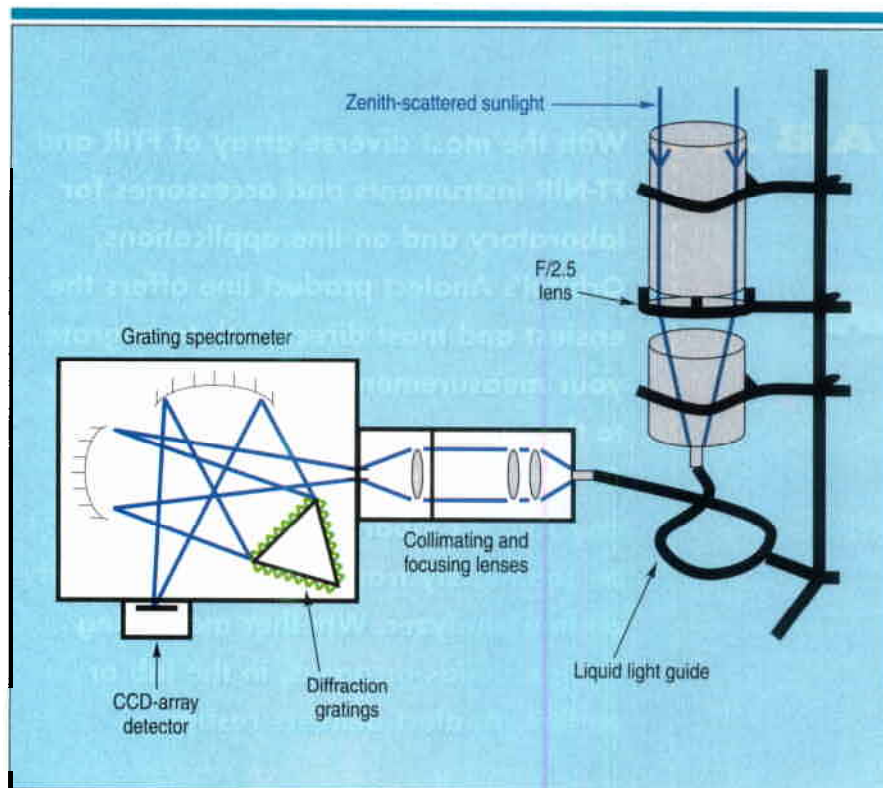


Figure 1. Instrumental set-up.

poorly understood and hard to replicate with computer models (4). Therefore, it is important to make high-quality measurements of stratospheric composition to monitor ozone concentrations and refine global climate models. Current indications suggest that increasing CO₂ concentrations will cool the stratosphere and enhance future Arctic losses on polar stratospheric clouds, with maximum ozone depletion predicted to occur during 2010–2019 (5).

To increase the geographic range and sampling density of ozone observations, we have constructed a portable ground-based spectrometer system capable of stand-alone measurements of ozone and a number of other trace stratospheric gases, including NO₂. The instrument was deployed in the high Arctic during the springs of 1999 and 2000 to monitor stratospheric composition during the critical period following polar sunrise.

EXPERIMENTAL SET-UP

A schematic diagram of the instrumental set-up is shown in Figure 1. In summary, a grating spectrometer fitted with a charge-coupled device (CCD) detector was used to record spectra of sunlight scattered from the zenith sky. All neces-

sary instrumentation was contained in a portable, thermostated aluminum trunk that is designed to withstand outdoor operation in harsh field environments such as the high Arctic, where temperatures regularly fall below -50 °C.

The aluminum trunk was fitted with a UV-grade Plexiglas window, oriented to allow zenith-scattered sunlight to enter the system. A fused-silica lens ($\phi = 40$ mm, $f/2.5$; Oriel Instruments, Stratford, CT) was used to focus incoming sunlight onto a liquid light guide (core $\phi = 3$ mm,

length = 1 m; Oriel Instruments). Emergent light from the light guide was then refocused onto the entrance slit of a TRIAX-180 imaging spectrometer (JY Horiba, Edison, NJ). The spectrometer was fitted with an adjustable entrance slit and a triple-grating turret (mounted with diffraction gratings of 400, 600, and 1800 grooves/mm) to ensure flexibility in the resolution and spectral range available. The resolution and bandwidth characteristics of each grating are summarized in Table I. A thermoelectrically cooled Spectrum 1 CCD array detector (with SITE chip 800 × 2000 pixels, each 15 μm × 15 μm) was mounted on the exit focal plane of the spectrometer. A CCD array was used instead of a diode-array detector to avoid artifacts introduced by signal-dependent dark current (6) and the Fabry-Pérot etalon structure that is inherent in many diode-array detectors (7). The CCD was back-illuminated to improve quantum efficiency of signal in the UV region, and on-chip binning of each pixel column was performed to maximize the signal-to-noise ratio.

Spectrometer control and data acquisition were automated using a customized LabVIEW program based on JY Horiba's instrument drivers. The system was operated using a laptop computer contained within the box, which resulted in a stand-alone instrument ideally suited for deployment in remote locations where ozone measurements are sparse. An additional feature of the system was the ability to control all instrumental settings and data collection from distant locations, using pcANYWHERE remote-access software (Symantec Corp., Cupertino, CA). This ability is especially useful for long-term monitoring at isolated sites, allow-

Table I. Spectral resolution and range of the TRIAX-180 grating spectrometer.

Grating (grooves/mm)	Spectral bandwidth (nm)	Entrance slit width (μm)	Resolution* (FWHM in nm)
400	360	50	2.0
		100	2.2
		200	2.9
600	234	50	0.9
		100	1.2
		200	1.8
1800	66	50	0.5
		100	0.6
		200	0.7

*Instrument resolution was determined by measuring the full width at half maximum (FWHM) of two mercury emission lines (436 and 546 nm), centered on the CCD array.

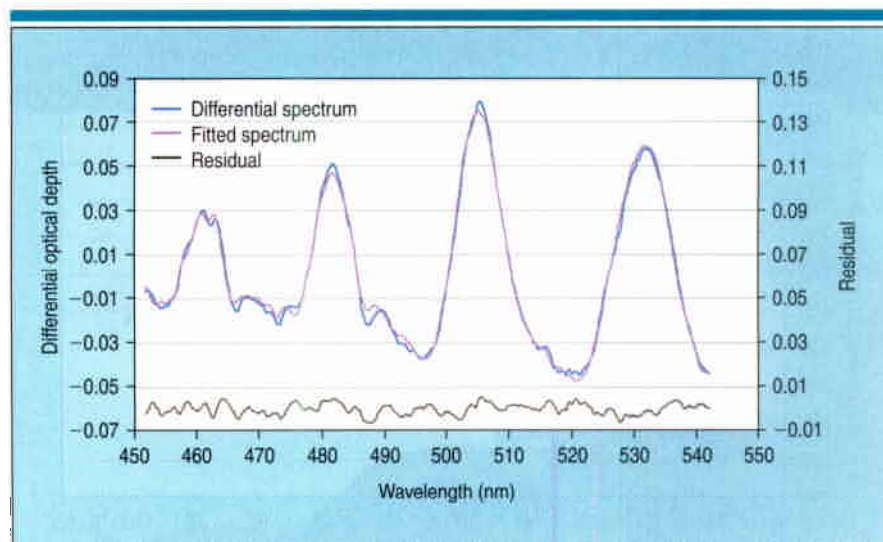


Figure 2. Observed and fitted optical depths in the ozone wavelength region.

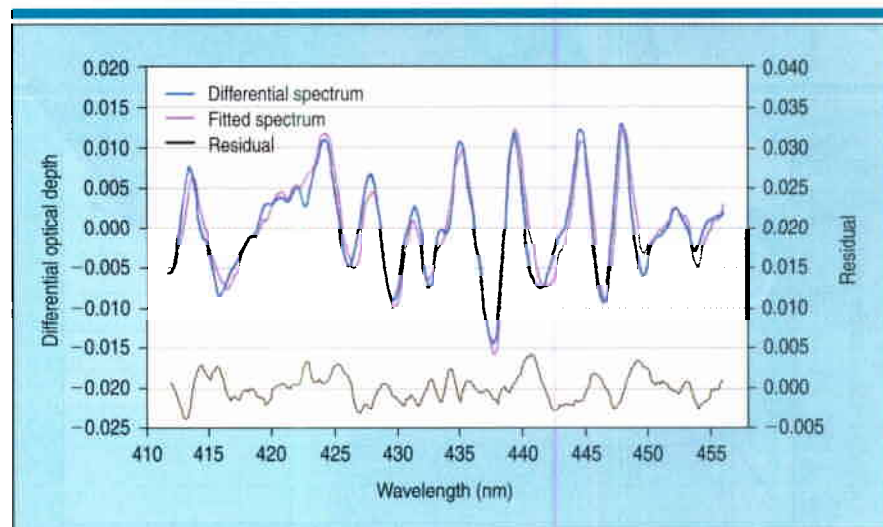


Figure 3. Observed and fitted optical depths in the NO_2 wavelength region.

ing the operator to remotely command the instrument.

RESULTS

During March–April 1999 and again in February–March 2000, the spectrometer was deployed at the Environment Canada Arctic Stratospheric Observatory, located in Eureka, Nunavut, Canada (80.1°N, 86.4°W). Stand-alone measurements of stratospheric gases were performed, which complemented those made by other instruments based at Eureka. Other instruments included a solar-tracking Fourier transform-infrared spectrometer, a nighttime lidar system, and frequent ozonesonde flights. Results from the 1999 campaign are presented here.

Zenith-sky spectra were recorded in the UV–visible region, typically between 320 nm and 554 nm, during each day from March 21 through April 21, 1999. Atmospheric column densities of gases with absorption features in this wavelength range were then retrieved from the spectra using differential optical absorption spectroscopy (DOAS) theory (8). In essence, DOAS uses the fact that scattered sunlight observed at twilight traverses a much longer stratospheric path than scattered sunlight at noon. For species with the bulk of absorbing molecules in the stratosphere (such as ozone and NO_2), the apparent slant column density is much greater in twilight spectra. The differential optical depth for each twilight measurement as a function of wave-

length, $OD(\lambda)$, was calculated from equation 1, where I and I_0 correspond to the intensity of the twilight and reference spectra respectively:

$$OD(\lambda) = -\ln \frac{I(\lambda)}{I_0(\lambda)} \quad (1)$$

The line-of-sight amount of each atmospheric absorber was retrieved by modeling $OD(\lambda)$, known as the differential spectrum. Differential cross-sections of absorption by ozone, NO_2 , O_4 , H_2O (and BrO and OCIO when present in the atmosphere), and of Rayleigh scattering were fitted to the differential zenith-sky spectrum using a simultaneous least squares algorithm. A correction for the Ring effect (9) was also included. Measured and fitted differential spectra for a typical twilight observation (April 5) during the Eureka campaign of 1999 are illustrated in Figures 2 and 3. The difference between the observed and fitted spectra is shown by the residual structure. A good indication of the quality of our results is the small magnitude of the residual structure compared with the observed spectra. Line-of-sight amounts (slant columns) of each absorber were converted to vertical column amounts by comparison with a model simulating the transfer of radiation through the atmosphere and associated photon path-lengths through a range of solar elevation angles (10).

Our 1999 ozone measurements are shown in Figure 4 alongside satellite observations made using the Total Ozone Mapping Spectrometer. It can be seen that there is good agreement between the two data sets, although the satellite measurements do not have the temporal resolution to discern short-term changes in ozone abundance over Eureka. Satellite and ground-based observations are complementary; the former provides a global picture, whereas the latter allows for long-term measurements at a particular site and the flexibility to move to different locations. Initial validation of our system was obtained during a field campaign at Vanscoy, Saskatchewan, Canada, in August 1998 where four independent sets of ozone column measurements were shown to agree to within 5%. Estimated errors on our measurements are <5% for ozone and 10–12% for NO_2 .

The NO_2 vertical column amounts for sunrise and sunset measurements are shown in Figure 5. A steady increase in

the total atmospheric column amount can be seen through the measurement period as the amount of sunlight increases with each day and the balance between NO_2 and the photochemically labile N_2O_5 shifts towards NO_2 . The difference between sunrise and sunset columns closes for the same reason. In fact, there was a linear relationship ($R^2 = 0.79$) between day length and the ratio of sunrise NO_2 columns to sunset columns.

SUMMARY AND CONCLUSIONS

The automated spectrometer system described in this article represents an additional instrument with which to monitor stratospheric ozone trends and provide new information on the mechanisms that cause ozone loss. It is ideally suited for stand-alone operation in remote locations and has proven to operate reliably during a four-week period at an Arctic site. Measurements have also been made at mid-latitude sites and an intercomparison exercise validated the accuracy of the new system.

We are now working on developing and implementing algorithms that will enable the retrieval of vertically resolved atmospheric concentration profiles from our ground-based observations. One other avenue of ongoing work is the optical coupling of a star-tracking telescope to the spectrometer to facilitate nighttime measurements of an increased number of atmospheric gases. This would allow measurements to be performed during the long polar night.

REFERENCES

- (1) J.C. Farman, B.G. Gardiner, and J.D. Shanklin, *Nature* **315**, 207–210 (1985).
- (2) R.C. Smith, R.B. Prezelin, K.S. Baker, R.R. Bidigare, N.P. Boucher, T. Coley, D. Karentz, S. MacIntyre, H.A. Matlick, D. Menzies, M. Ondrusek, Z. Wan, and K.J. Waters, *Science* **255**, 952–959 (1992).
- (3) D.P. Donovan, H. Fast, Y. Makino, J.C. Bird, A.I. Carswell, J. Davies, T.J. Duck, J.W. Kaminski, C.T. McElroy, R.L. Mittermeier, S.R. Pal, V. Savastouk, D. Velkov, and J.A. Whiteway, *Geophys. Res. Lett.* **24**, 2709–2712 (1997).
- (4) World Meteorological Organization, *Scientific Assessment of Ozone Depletion: 1998* (Report No. 44, Global Ozone Research and Monitoring Project: WMO, Geneva, 1999), pp. 7.47–7.53.
- (5) D.T. Shindell, D. Rind, and P. Lonergan, *Nature* **392**, 589–592 (1998).
- (6) U. Platt, L. Marquard, T. Wagner, and D. Perner, *Geophys. Res. Lett.* **24**, 1759–1762 (1997).

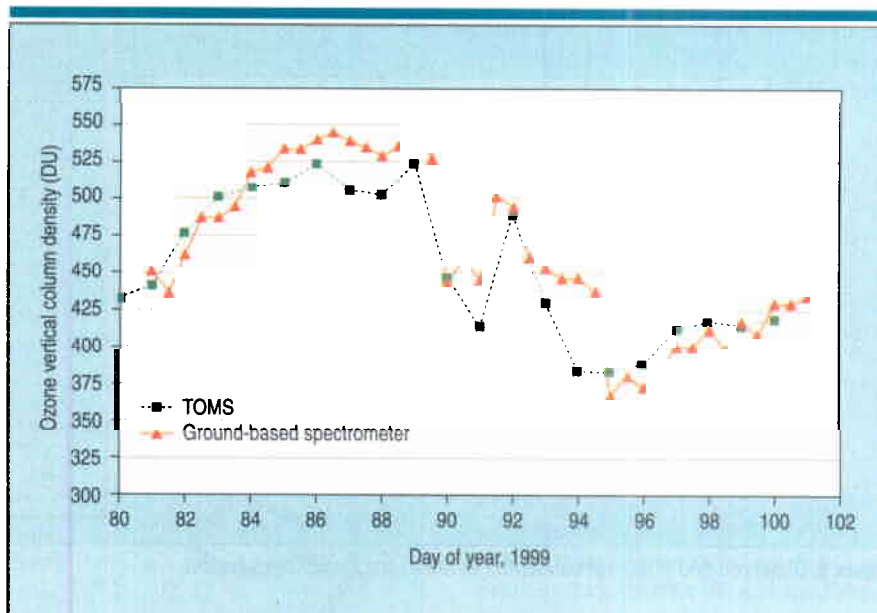


Figure 4. Ozone measurements over Eureka during spring 1999.

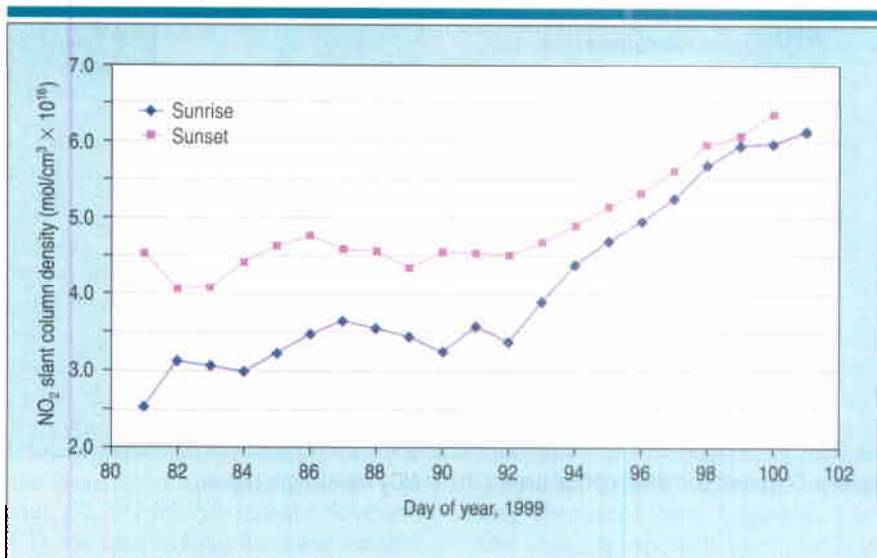


Figure 5. NO_2 Slant column amounts ($\text{SZA} = 90^\circ$) over Eureka during spring 1999.

- (7) G.H. Mount, R.W. Sanders, and J.W. Brault, *Appl. Optics* **100**, 851–858 (1992).
- (8) S. Solomon, A.L. Schmeltekopf, and R.W. Sanders, *J. Geophys. Res.* **92**, 8311–8319 (1987).
- (9) K.V. Chance and R.J.D. Spurr, *Appl. Optics* **36**, 5224–5230 (1997).
- (10) C.A. McLinden, *Observation of atmospheric composition from NASA ER-2 spectroradiometer measurements* (Ph.D. thesis, York University, Toronto, Canada, 1998) p. 292.

Matthew R. Bassford is a postdoctoral fellow and Kimberly Strong is an assistant professor in the Department of Physics, University of Toronto, 60 St. George Street, Toronto, ON, Canada M5S 1A7. Correspondence should be addressed to Strong; she may be contacted by phone at (416) 946-3217, by fax at (416) 978-8905, and by e-mail at strong@atmosph.physics.utoronto.ca. Jagdish Rebello is detector product manager in the Optical Systems Group at JY Horiba, 3880 Park Avenue, Edison, NJ 08820, USA. ♦